Eur Biophys J (1998) 27: 247–254

ARTICLE

A. Reginald Waldeck · Arron S.-L. Xu
Basil D. Roufogalis · Philip W. Kuchel

NMR measurements of Ca^{2+} and H^+ transport mediated by A23187 and reconstituted plasma membrane Ca^{2+}-ATPase

Received: 19 June 1997 / Accepted: 3 December 1997

Abstract NMR-based assays for measuring the fluxes of Ca^{2+}, H^+, and ATP in liposomal systems are presented. The ^{19}F NMR Ca^{2+}-chelating molecule 5,5-difluoro-1,2-bis(*o*-amino-phenoxy)ethane-N,N,N′,N′-tetraacetic acid (5FBAPTA) was trapped inside large unilamellar vesicles and used to monitor passive and A23187-mediated Ca^{2+} transport into them. The data were analyzed using progress curves of the transport reaction. They demonstrated the general applicability of 5FBAPTA as a ^{19}F NMR probe of active Ca^{2+} transport. ^{31}P NMR time-courses were used to monitor *simultaneously* the ATP hydrolysing activity of the reconstituted human erythrocyte Ca^{2+}-ATPase and the concomitant acidification of the reaction medium in a suspension of small unilamellar vesicles. Using an estimate of the extraliposomal buffering capacity, the H^+/ATP coupling stoichiometry, in the presence of A23187, was estimated from the NMR-derived data at steady state; it amounted to 1.4 ± 0.3. This result is discussed with respect to the issue of molecular 'slip' in the context of a non-equilibrium thermodynamics model of the pump (accompanying paper in this issue). Importantly, NMR, in contrast to optical detection methods, can potentially register all fluxes and (electro)chemical gradients involved in the Ca^{2+}-ATPase-mediated H^+/Ca^{2+}counterport, in a single experiment.

Key words NMR · 5FBAPTA · Electrogenicity · Slip · Coupling stoichiometry

A. R. Waldeck[1] · A. S-L. Xu[2] · P. W. Kuchel (✉)
Department of Biochemistry, The University of Sydney, Sydney 2006, N.S.W, Australia
(e-mail: P. Kuchel@biochem.usyd.edu.au)

B. D. Roufogalis
Department of Pharmacy, The University of Sydney, Sydney 2006, N.S.W., Australia

Present addresses:
[1] Biochemistry Unit, The Heart Research Institute, 145-147 Missenden Road, Camperdown 2050, N.S.W., Australia
[2] MD4A-01, Laboratory of Structural Biology, National Institute of Environmental Health Sciences, P.O. Box 12233, Research Triangle Park, NC 27709-2233, USA

Abbreviations *5FBAPTA* 5,5-difluoro-1,2-bis(*o*-aminophenoxy)ethane-N,N,N′,N′-tetraacetic acid · *EDTA* Ethylenediaaminetetraacetic acid · *FCCP* Carbonylcyanide-*p*-trifluoromethoxy-hydrazone · *Hepes* 4-(2-hydroxyethyl)-1-piperazineethanesulfonate · *LUV* Large unilamellar vesicles · *MDP* Methylene diphosphonate · *MeP* Methylphosphonate · *MLV* Multilamellar vesicles · *β-NADH* Nicotinamide adenine dinucleotide · *NET* Non-equilibrium thermodynamics · *NMR* Nuclear magnetic resonance · *SD* Standard deviation · *SE* Standard error · *SUV* Small unilamellar vesicles · T_1 Spin-lattice relaxation time · *Quin-2* 2-[(2-bis-[carboxymethyl]amine-5-methylphenoxy)-methyl]-6-methoxy-8-bis[carboxymethyl]aminoquinoline

Introduction

NMR is a powerful analytical tool for the measurement of ionophore-mediated and passive transport of ions and non-electrolytes in cells and liposomes (for reviews see Grandjean and Laszlo 1987; Kuchel et al. 1994). ^{19}F NMR, in conjunction with a variety of fluorinated Ca^{2+}-chelating molecules, has been employed to measure the free intracellular Ca^{2+} concentration (Levy et al. 1987) in erythrocytes (Gilboa et al. 1994), perfused rat heart (Steenbergen et al. 1987), and actively metabolising cerebral tissue (Bachelard et al. 1988). ^1H, ^{13}C, and ^{31}P NMR have had long-standing use in the study of the energy metabolism of organelles and cells. ^{31}P NMR, particularly, has been used extensively because it can monitor *non-invasively* intracellular ATP, ADP, and P_i concentrations in conjunction with intra- and extracellular pH (Nicolay et al. 1981, 1983; Lundberg et al. 1990). The values of the coupling stoichiometries characterising the bioenergetic action of the lactate/proton carrier of *Streptococcus faecalis* (Simpson et al. 1983) and the ATP-synthase of *Escherichia coli* (Vink et al. 1984) have been estimated employing ^{31}P NMR methods.

In this work we describe the novel application of NMR spectroscopy to study passive and A23187-induced uptake of Ca^{2+} ions in LUV using the probe-molecule 5-^{19}FBAPTA. These experiments form the basis for future measurements of active Ca^{2+} transport in LUV. ^{31}P NMR time-course measurements were used to study the ATP-driven proton-ejection activity of the reconstituted ion pump. The ATP hydrolysing activity of the pump and the extraliposomal pH were monitored within the same ^{31}P NMR experiment. Data derived from these experiments, and an estimate of the buffering capacity of the suspending medium, were used to calculate the H^+/ATP coupling stoichiometry (n_P^H) at a steady state, in the presence of a saturating concentration of A23187. $n_P^H = 1.4 \pm 0.3$, is in reasonable agreement with $n_P^H = 1$, measured under *pre*-steady state conditions in LUV (Hao et al. 1994). This finding is discussed in more detail within the context of a NET model of a slipping Ca^{2+}-ATPase (accompanying paper in this issue).

Materials and methods

Materials

Centricon microconcentrators (cut-off 30 kDa) were obtained from Amicon, Danvers, CT. ^2H_2O was obtained from the Australian Institute for Nuclear Science and Technology, Lucas Heights, NSW, Australia. Phospholipids from soybeans (asolectin) were obtained from MCB Manufacturing Chemical Inc., Cincinnati, OH. All other chemicals were of AR grade.

Preparation of liposomes and proteoliposomes

LUV were prepared from 50 mg L-α-phosphatidylcholine (from egg yolk) in 1 ml buffer containing 50 mM KCl, 20 mM K-Hepes, and 10 mM 5FBAPTA (potassium salt) pH 7.4, and 4 ml diethyl ether, by the reverse-phase evaporation technique (Szoka and Papahadjopoulos 1978). The external 5FBAPTA was dialyzed away completely against 3 l (one buffer change) of the same buffer without 5FBAPTA. Tonicity of the dialysis buffer was maintained by the inclusion of sucrose.

The plasma membrane Ca^{2+}-ATPase was purified from human erythrocytes as described previously (Villalobo and Roufogalis 1986; Roufogalis and Villalobo 1989) with minor modifications. The batches of purified enzyme were collected in 20% glycerol, 15 mM Hepes, and 200 mM KCl, pH 7.4. Proteoliposomes (SUV) were prepared by a cholate dialysis method, and protein determinations were performed according to a modified Lowry procedure, as described in Villalobo and Roufogalis (1986). The NMR sample (SUV; pH 7.4) contained 15 mg ml^{-1} lipid, ~40 mg ml^{-1} protein, 100 mM KCl, 10 mM Hepes, 5 mM $MgCl_2$, 1 mM dithiothreitol, and 50 μM $CaCl_2$.

Experimental procedures

The ATP hydrolysing activity of the proteoliposomes and the stimulation of this activity by A23187 were determined routinely by following the oxidation of β-NADH at a wavelength of 340 nm on a Varian Cary 3 spectrophotometer, in the presence of an ATP-regenerating system, as described previously (Villalobo and Roufogalis 1986).

Passive and ionophore Ca^{2+} transport were initiated by the addition of 3.5 mM $CaCl_2$ (final concentration with respect to the total volume of the suspension). Further experimental details are given in the legend of Fig. 1.

The suspension of proteoliposomes used in the ^{31}P NMR experiment (Figs. 2 and 3) was concentrated into a final volume of ~2 ml by centrifugation (3080 g; 60 min; ~278 K) in microconcentrators, and the suspension was placed in a 10-mm NMR tube. See the legend of Fig. 2 for more experimental detail.

The pH calibration experiment (data not shown) was performed on a 3 ml sample containing reconstitution buffer (*vide supra*) which was supplemented with ATP (5 mM), MeP (5 mM), P_i(mM), and 15 mg ml^{-1} dispersed asolectin SUV. The buffering capacity of the extraliposomal medium was estimated, as previously (Mitchell and Moyle 1967) over the pH range 7.0–7.4 in a suspension of 15 mg ml^{-1} dispersed asolectin (data not shown). The buffer was of the same composition as that which was used for the time-course experiments (i.e., reconstitution buffer supplemented with 5 mM MeP and 3.5 mM ATP) at 310 K; 2 μM (final concentration) FCCP was added to dissipate any pH gradients that may have developed.

NMR methods

^{19}F NMR equilibrium magnetization spectra of 5FBAPTA trapped inside LUV were acquired with a spectral width of 6,850 Hz over 8 k data points using an intertransient delay of 4.6 s (>5 T_1; see Table 1), and averaged over 32 transients. ^{19}F NMR time-course measurements of Ca^{2+} influx into the LUV were recorded using the same spectral width and digitization parameters and averaged over the same number of transients, but with a 45° rf pulse (14–15 μs) and an intertransient delay of 1.1 s (>1 T_1). ^{31}P NMR time-course measurements were recorded using a spectral width of 10,630 Hz over 8 k data points, a 70° rf pulse (~15 μs), and intertransient delay of 1 s (~1 T_1), and averaged over 512 transients. The extent of sample heating, due to proton decoupling was measured by using the shift of ethylene glycol in a glass capillary inserted coaxially in the NMR tube (Bubb et al. 1988), and the probe-thermosat setting was adjusted accordingly.

Analysis of Ca-5FBAPTA and 5FBAPTA data of Ca^{2+}-transport in LUV

The Ca-5FBAPTA and 5FBAPTA time-course experiments were analyzed using progress curve analysis, essen-

tially as described previously (Erdahl et al. 1994, 1995):

$$I(t) = I_0 + A\,t + B\,t^2 \quad (1)$$

$$I(t) = I_m^2\,k\,t/(1 + I_m\,k\,t) \quad (2)$$

$$I(t) = I_m\,(1 - \mathrm{Exp}[-k\,t]) \quad (3)$$

where, in Eq. (1), I and I_0 denote peak-integral and its initial value at t = 0, respectively; A denotes the initial rate of Ca^{2+} influx, and B is a correction factor for non-linearity. In Eqs. (2) and (3), k denotes the apparent rate constant, and the subscript m denotes maximum, or minimum, for Ca-5FBAPTA and FBAPTA data, respectively. Equations (1)–(3) are valid for the analysis of the monotonically increasing Ca-5FBAPTA data. The 5FBAPTA peak-integrals decay with time (see Fig. 1C); thus, Eqs. (1)–(3) were modified accordingly.

The exchange reaction between free and FBAPTA-chelated (bound) Ca^{2+}, present in the intraliposomal compartment only (see cartoon in Fig. 1A) is governed by the following equilibrium (Gilboa et al. 1994):

$$\text{Ca-5FBAPTA} \underset{k_{on}}{\overset{k_{off}}{\rightleftharpoons}} Ca^{2+} + \text{FBAPTA} \quad (4a)$$

with

$$K_d = \frac{k_{off}}{k_{on}} = \frac{[Ca^{2+}][\text{5FBAPTA}]}{[\text{Ca} - \text{5FBAPTA}]} \quad (4b)$$

The intraliposomal 5FBAPTA and Ca-5BAPTA concentrations (at time t) were calculated as follows:

$$[\text{5FBAPTA}] = \left(\frac{I_{\text{5FBAPTA}}}{(I_{\text{5FBAPTA}} + I_{\text{Ca-5FBAPTA}}}\right) \cdot ([\text{5FBAPTA}] + [\text{Ca} - \text{5FBAPTA}]) \quad (5a)$$

$$[\text{Ca} - \text{5FBAPTA}] = \left(\frac{I_{\text{Ca-5FBAPTA}}}{I_{\text{5FBAPTA}} + I_{I_{\text{Ca-5FBAPTA}}}}\right) \cdot ([\text{5FBAPTA}] + [\text{Ca} - \text{5FBAPTA}]) \quad (5b)$$

where ([Ca-5FBAPTA] + [5FBAPTA]) = 10 mM (see Materials and methods). Thus, the concentration of free and bound intraliposomal Ca^{2+} may be calculated directly from the values of the 5FBAPTA and Ca-5FBAPTA NMR peak-integrals and a knowledge of K_d (708 nM; Metcalfe et al.1985), via Eqs. (4b), (5a) and (5b). The extraliposomal concentration at time t was estimated using the condition of mass-conservation, as follows:

$$[Ca^{2+}]_e = \left(\frac{[Ca^{2+}]_{total} - [Ca]_{i,bound}\,V_i^f}{V_e^f}\right) \quad (6)$$

where V_i^f and V_e^f are the internal (0.35) and external (0.65) volume fractions (Waldeck and Kuchel 1993), and we have recognized that $[Ca^{2+}]_{i,bound} \gg [Ca^{2+}]_{i,free}$ (see legend of Fig. 1).

Analysis of pH time-courses using MeP and P_i in Ca^{2+}-ATPase SUV

The Henderson-Hasselbalch equation modified for an NMR titratable species was used to convert the chemical shifts of the MeP and P_i resonances (data not shown), as described previously (Stewart et al. 1986).

Estimation of the H^+/ATP coupling stoichiometry in the presence of A23187

The stoichiometry factor n_P^H is the ratio of the rates of vectorial proton flow, J_P^H, to that of ATP hydrolysis, J_P; and it was calculated for ATPase-mediated H^+/Ca^{2+} counterport in the presence of a saturating concentration of A23187 at steady state. The rate of the total proton production in the extravesicular medium, J_H^e, is the sum of the rates of production of scalar H^+, J_H^s, and vectorial H^+, J_P^H . $n_P^{H,s}$ denotes the number of scalar H^+ that are produced per molecule of ATP hydrolyzed (0.8 at pH 7.2–7.4 in the presence of Mg^{2+}; Nishimura et al. 1962); $n_{Ca}^{H,A}$ denotes the number of H^+ counterported inwards per Ca^{2+} extruded by A23187 (2; Erdahl et al. 1994, 1995) as a result of Ca^{2+} pumping, respectively. It is the quantity J_H^e that was measured indirectly in the NMR experiments as the rate of change of pH of the extravesicular medium, i.e., $\Delta pH_e/\Delta t$ ($\approx \delta pH_e/\delta t$); the latter quantity is multiplied by the buffering capacity of the extraliposomal medium, β_e, to yield the former. From these considerations (see also Fig. 1 in accompanying paper in this issue), we derived an expression of n_P^H measured in the presence of A23187:

$$n_P^H = \frac{J_P^H}{J_P} = \left(\frac{J_H^e - J_H^s}{J_P}\right) - n_{Ca}^{H,A} \quad (7a)$$

with

$$J_H^e = -\beta_e \times \left(-\frac{\delta pH_e}{\delta t}\right) \approx \left(\frac{\Delta H_e^+}{\Delta pH_e}\right)\left(\frac{\Delta pH_e}{\Delta t}\right) \quad (7b)$$

and

$$J_H^s = n_P^{H,s} \times J_P \quad (7c)$$

Numerical procedures

Non-linear least-squares regression analysis was performed using the computer program Regression on a Macintosh FX computer. The SD of J_P and J_H^e were calculated by propagation of the errors in the MDP spectral integral and the protein concentration, and in the protein concentration alone, respectively. The SD of n_P^H was calculated by propagation of the errors in $\Delta pH_e/\Delta t$ and J_P.

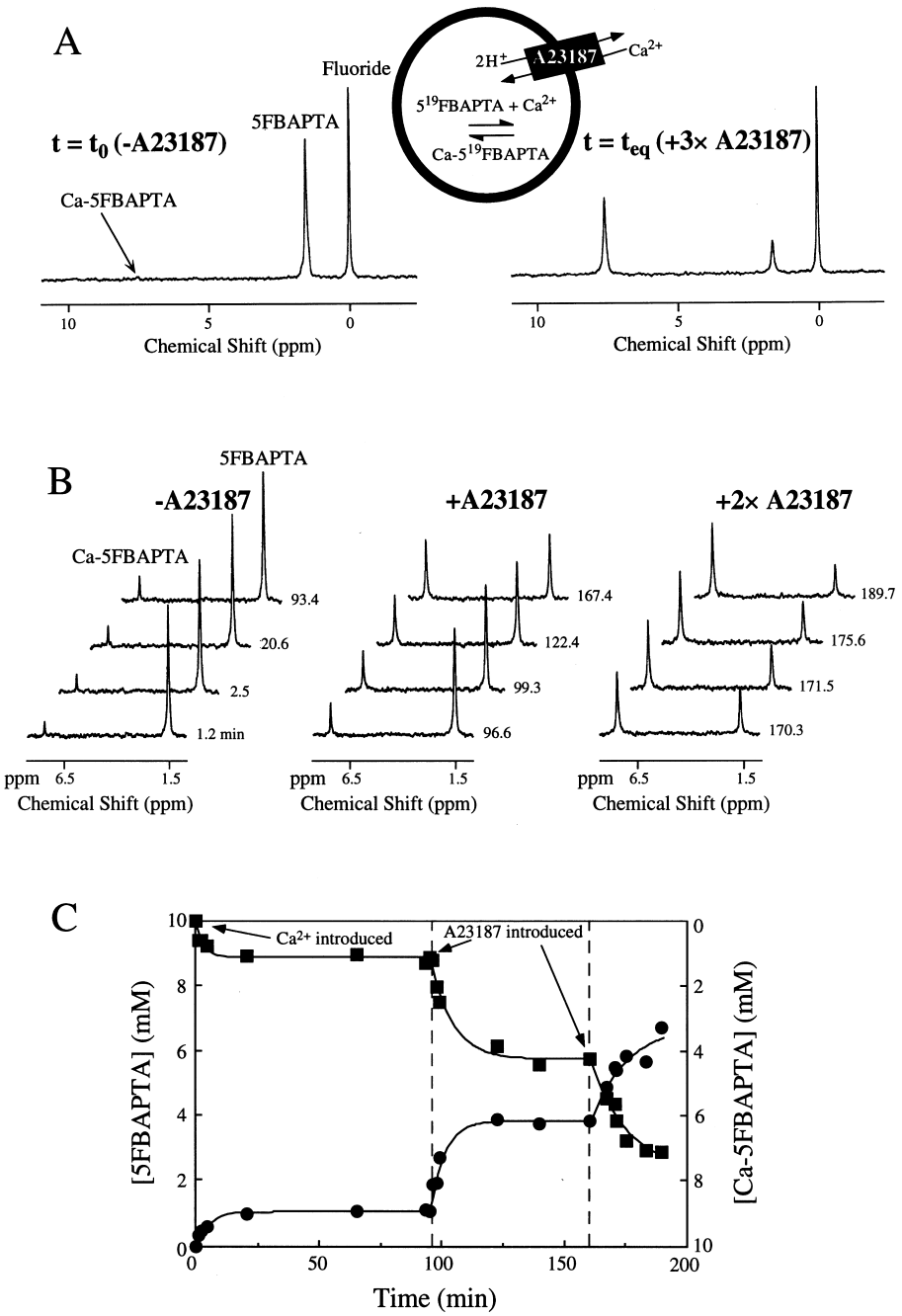

Fig. 1A–C ^{19}F NMR spectra acquired prior to the addition of Ca^{2+} and after Ca^{2+} had equilibrated across the membrane; see cartoon for a schematic representation of the transport system. The *arrow* in **A** indicates the Ca-5FBAPTA peak, and it corresponds to ~10 μM intraliposomal Ca^{2+} originating from the stock solution of PC. NaF (100 mM) in a 2 mm o.d. coaxial capillary as a chemical shift and intensity reference was arbitrarily set to 0.000 ppm. The chemical shift difference between the resonances corresponding to Ca-5FBAPTA and 5FBAPTA was 5.95 ppm. The fluoride resonance was at 1.62 ppm to lower frequency of the 5FBAPTA resonance. The linewidths for the Ca-5FBAPTA, 5FBAPTA, and F^- resonances were 26 Hz, 30 Hz, and 12 Hz, respectively. **B** Twelve of the 46 proton-decoupled ^{19}F NMR spectra of LUV-entrapped 5FBAPTA (initially 10 mM) acquired over ~190 min, at 298 K in the absence and presence of A23187 (9 μM additions). The time to the mid-point of accumulating each spectrum is given on the right-hand side of the corresponding spectrum. A linebroadening factor of 10 Hz had been (routinely) applied to each free induction decay prior to Fourier transformation. **C** Graph of the time-course 5FBAPTA (*squares*) and Ca-5FBAPTA (*circles*) peak-integrals normalized to those of fluoride and set to 10 and 0 mM at t = 0, respectively (data from **B**). The best fits obtained from non-linear least-squares regression of Eq. 3 onto the Ca-5FBAPTA and 5FBAPTA peak-integrals are shown. Concentrations immediately after the introduction of A23187, at the times indicated, (*dotted lines*) were: $[Ca^{2+}]_{i,bound}$ = 1.07 mM, $[Ca^{2+}]_{i,free}$ = 85 nM, and $[Ca^{2+}]_e$ = 4.81 mM after the first addition, and $[Ca^{2+}]_{i,bound}$ = 4.22 mM, $[Ca^{2+}]_{i,free}$ = 516 nM and $[Ca^{2+}]_e$ = 2.83 mM, after the second addition, respectively. The combined integrals of 5FBAPTA and Ca-5FBAPTA, and that of fluoride during the time-course were 118 ± 4 arbitrary units (a.u.) and 10 ± 3 a.u., respectively

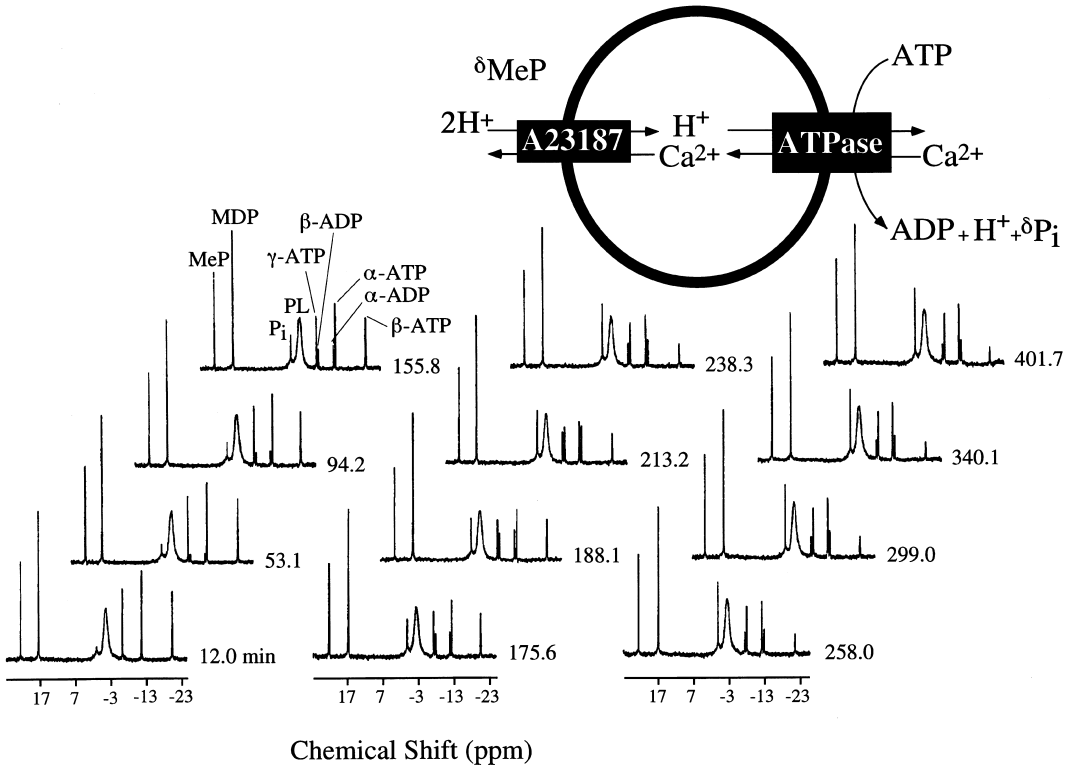

Fig. 2 Twelve of the 22 proton-decoupled ^{31}P NMR spectra acquired over 402 min, demonstrating coupled, A23187-uncoupled (187 μM), and orthovanadate-inhibited (5 μM) ATP hydrolysing activity in a suspension of Ca^{2+}-ATPase liposomes, at 310 K. The time-midpoint of acquisition of each spectrum is given on its right side; see cartoon for a schematic representation of the transport system. Calmodulin (240 nM final concentration) was added to activate the enzyme. ATP hydrolysis was initiated by the addition of ATP to a final concentration of 3.5 mM. Untitrated MDP (140 mM in ^2H_2O) in a cylindrical glass capillary (2 mm o.d.) was placed coaxially in the 10-mm NMR tube; it served as a chemical shift and intensity reference. The sample was field-frequency locked on the ^2H_2O present in the capillary. MeP (5 mM final concentration) was added to the contents of the 10-mm NMR tube to register the extravesicular pH. The chemical shifts of the ^{31}P NMR resonances were referenced to (external) 85% orthophosphoric acid. **A** A linebroadening factor of 5 Hz was applied to the free induction decays prior to their Fourier transformation

Table 1 ^{19}F NMR longitudinal relaxation times (T_1) of FBAPTA and Ca-FBAPTA in buffer and LUV[a]

Medium	$T_1 \pm$SD (ms)	
	Ca-FBAPTA	FBAPTA
buffer $-Ca^{2+}$		824.7±14.2
buffer $+Ca^{2+}$	775±64	813 ±47
LUV $-Ca^{2+}$		860.9±11.2
LUV $+Ca^{2+}$	868±51	783.1±17.6

[a] 50 mM KCl, 20 mM Hepes, and 5 mM FBAPTA, in the presence and absence of 2.5mM $CaCl_2$. LUV were prepared in the same buffer with or without 2mM $CaCl_2$

Results

Passive and ionophore-mediated Ca^{2+} transport in LUV

Figure 1A shows ^{19}F NMR equilibrium magnetization spectra of 5FBAPTA and Ca-5FBAPTA trapped in LUV (see inset reaction sheme); the spectra were acquired before the addition of Ca^{2+} ($t=t_0$), and at equilibrium ($t=t_{eq}$; after the time-course experiment; see panel B). The similarity of the T_1's of the 'free' and Ca^{2+}-complexed 5FBAPTA (see Table 1) allowed quantification under 'rapid pulsing' conditions (see NMR Methods). Panel C shows a graph of the peak-integrals versus time of the 5-FBAPTA and Ca-5FBAPTA resonances (B) normalized against those of the fluoride standard and 5FBAPTA concentration at $t=0$; i.e., 10 mM. The solid lines are the 'best fits' of Eq. (3) onto the data. The estimates of the initial rates of Ca^{2+} influx (A; Eq. (1)) and the extents of the reactions (I_m; Eq. (2)) are given in Table 2 together with the estimates of the apparent rate constants (k; Eq. (3); also see Discussion). The apparent paradox that the rate of Ca^{2+} entry decreases with successive additions of A23187 has been reported previously (Erdahl et al. 1994, 1995) and is explained in the Discussion.

The ATP hydrolysing activity and extravesicular pH in Ca^{2+}-ATPase SUV

Figure 2 shows stackplots of ^{31}P NMR spectra demonstrating ATP hydrolysing activity in a suspension of Ca^{2+}-AT-

Table 2 Apparent rate constants, extents of transport, and initial rates of Ca^{2+} flux into LUV measured by the rise of Ca-5FBAPTA and decay of the 5FBAPTA resonances in the absence and presence of A23187 (Fig. 1), and analyzed by fitting appropriate portions of the data (see Eqs. (1)–(3))

Ca5-FBAPTA	5FBAPTA	k ($10^4 \times s^{-1}$)	Extent (%)[a]	Rate ($\mu M\ s^{-1}$)
Passive		35±5	11.7±0.3	2.5±0.5
+A23187[b]		29±6	44±2	4.6±1.3
+2×A23187[b]		12±6	84±11	2.0±0.3
	Passive	57±22	7.9±0.9	1.9±0.9
	+A23187[b]	19±7	42±10	4.5±1.6
	+2×A23187[b]	9±4	101±29	1.8±0.3

[a] The extent of transport is given as a percentage of the total FBAPTA peak-integral; i.e., $I_{Ca\text{-}5FBAPTA} + I_{5FBAPTA}$

[b] Addition of 9 μM (final concentration)

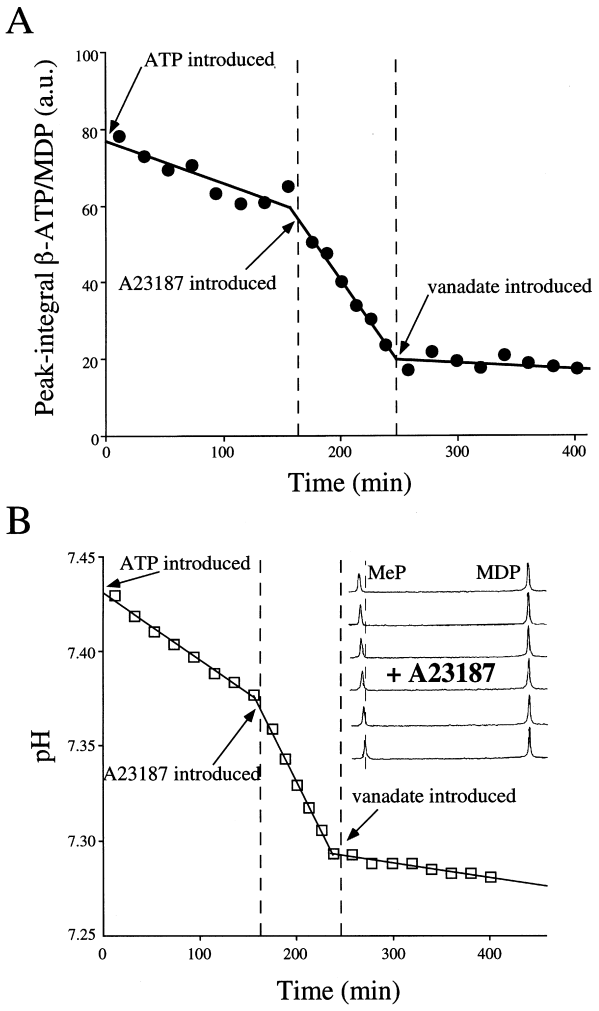

Fig. 3 **A** Graph of the decay of the β-ATP resonance normalized to the peak-integral of MDP, with time, from the data presented in Fig. 2. The times of addition of the ionophore and inhibitor are shown by the *dotted lines*. ATP, ADP, and P_i concentrations immediately after the introduction of A23187 were 2.5 mM, 0.5 mM, and 0.5 mM, respectively; the concentrations immediately after the addition of orthovanadate were 0.9 mM, 1.3 mM, and 1.3 mM, respectively. The integral of the resonance corresponding to MDP remained relatively constant at I=98±4 a.u., (n=22); its chemical shift remained constant during the entire time-course (see inset to Fig. 3B). **B** Graph of the time-dependent decrease in the pH of the extraliposomal medium registered by the change in the chemical shift of MeP referenced to MDP from the time-course data depicted in Fig. 2. The times of addition of the ionophore and inhibitor are indicated by the *dotted lines*. The pH-values immediately after addition of ATP, A23187, and orthovanadate were 7.43, 7.37 and 7.29, respectively. The inset depicts stackplots of the chemical shifts of MeP with respect to MDP in the presence of A23817 (enlargements of the spectra shown in Fig. 2)

Pase liposomes at 310 K in the absence and presence of A23187 and orthovanadate.

Figure 3A shows a graph of the time-course data obtained from the spectra in Fig. 3. The coupled (–A23187), (partially) uncoupled (+A23187), and inhibited (+orthovanadate) rates of ATP hydrolysis were 166±26, 670±104, and 15±3 nmol (mg protein)$^{-1}$ min^{-1}, respectively. Thus the uncoupler-stimulation-factor estimated from these data was 4.0 (670/166). The measured rates were corrected for the fraction of ATPases (~20%) with their catalytic sites in the interior of the liposomes (Wang et al. 1989).

Figure 3B shows a graph of the decrease in the pH of the medium caused by the scalar and vectorial proton production of the reconstituted Ca^{2+}-ATPase versus time registered by MeP (data from Fig. 2). The uncoupler-stimulation factors that were estimated from the chemical shifts of P_i and MeP were 3.5 and 2.9, respectively. The total proton production rates in the extravesicular medium (J_H^e; Eq. (7b)) in the absence, and presence of A23187, and presence of A23187 and orthovanadate, were 58±9, 164±25, and 11±1 nmol mg^{-1} min^{-1}, respectively. The P_i peaks became shifted to lower frequency (data not shown), and that of the MeP peak to higher frequency (see inset for spectra in the presence of A23187); both are consistent with the activity of the pump resulting in acidification of the extraliposomal medium.

The H^+/ATP coupling stoichiometry

n_P^H in the presence of A23187 was estimated at steady state from Eqs. (7a–c), and it amounted to 1.4±0.3. β_e amounted to 10 μM H^+/pH unit (data not shown); $\Delta pH_e/\Delta t$ in the presence of A23187 was estimated to be 1×10^{-3} pH unit min^{-1} (see inset of Fig. 3B).

Discussion

Measurement of passive and A23187-mediated Ca^{2+} transport

Our experiments showed that the ^{19}F NMR Ca^{2+}-probe 5-FBAPTA could be used to measure rates of passive and ionophore-facilitated diffusion of Ca^{2+} ions across the

membranes of LUV. Therefore, these measurements encourage further NMR studies of ATPase-mediated Ca^{2+}-pumping.

Two particular features of the Ca-$A23187_2$ transport system are revealed by the progress curve analysis [Fig. 1C and Eqs. (1)–(3)]. First, increasing the ionophore concentration in the membranes brought about by the second addition of A23187 did not produce the expected increase in the initial rate (see Table 2). This phenomenon has previously been observed by fluorescence spectroscopy in Quin-2-loaded liposomes (Erdahl et al. 1994, 1995). The authors extensively characterized this transport system, and their explanation applies to our experiments as follows: the internal pH rises as A23187-mediated Ca^{2+}/H^+ counterport proceeds, resulting in the build-up of an inside-basic ΔpH. This causes the $A23187^-$ to accumulate in the *internal* leaflets of the membranes, because the anionic form of the ionophore is membrane-impermeable. That is, the intraliposomal H^+ concentration becomes the restricting factor promoting the A23187 redistribution to the *exo*facial side of the membranes. Thus, the otherwise expected increase in the rate of influx of Ca^{2+} with successive additions of the ionophore does not occur, because of the relative decrease in concentration of the transporting species ($A23187_2$-Ca) on the exofacial side of the membrane. Second, the ΔpH effect limits the extent of the reaction, and therefore becomes a function of the A23187 concentration (see Table 2).

Measurement of reconstituted Ca^{2+}-ATPase activity

It has been shown that the ATP hydrolysing activity and the concomitant total extraliposomal proton production in SUV containing the plasma membrane Ca^{2+}-ATPase is registered quantitatively by the ^{31}P NMR method. Simultaneous fluorescence measurements have been reported, but these have been (are) limited to dual-wavelength recordings (Karon et al. 1995), excluding future measurement of all three of ATP hydrolysis, Ca^{2+} pumping, and H^+ ejection and their associated forces. Reconstituting the Ca^{2+}-pump into LUV (Yu et al. 1993; Hao et al. 1994) should now enable the simultaneous NMR detection of the steady state flows and 'forces' (electrochemical gradients) involved with its action, in a single sample by devising 'interleaved' experiments and making use of the nuclei ^1H, ^{19}F, and ^{31}P. The former may be used to register *intra*vesicular pH and changes in Ca^{2+} concentration in conjunction with EDTA (Yoon and Sharp 1985). ^{19}F NMR may be employed in conjunction with fluoroanilines (Deutsch and Taylor 1989) to measure ΔpH. Novel ^{19}F NMR procedures employing membrane potential probe-molecules (Xu and Kuchel 1991) may be developed concurrently to enable quantification of $\Delta\psi$ in liposomal systems.

The pH registered by MeP (see inset of Fig. 3B) has been used for quantification of J_H^e because the pK'_a of MeP (7.76) was closer to the pH of the suspension (data not shown); thus, estimates of pH made using the MeP titation curve would be more precise and accurate than for P_i. Also, MeP (>1– charge; pH 7.3–7.4) and P_i (>1.5– charge; pH>6.8) are very membrane impermeable. In the event that some external MeP would have permeated, its transmembrane exchange rate would almost certainly have been slow on the NMR time-scale (Stewart et al. 1986), thus resulting in separate intra- (<5%) and extravesicular (>95%) MeP resonances. Thus, any intraliposomal MeP would not have interfered with the measurement of pH_e by registering an average pH (chemical shift) weighted by the relative internal and external population fractions.

Bioenergetic implications

Our finding that $n_P^H = 1.4 \pm 0.3$ constitutes both the first NMR, and steady state measurement of a coupling stoichiometry in a proteoliposomal suspension. It is in reasonable agreement with that of Hao et al. (1994), who found $n_P^H = n_P^{Ca} = 1$ under "optimal" conditions (i.e., early time of reaction in the presence of calmodulin; $n_P^{Ca} = Ca^{2+}/ATP$) in LUV.

It has been proposed that the plasma membrane Ca^{2+}-ATPase is subject to molecular slip; i.e., catalytic turnover failing to result in vectorial displacement of bound cation. On a molecular level, n_{Ca}^H is likely to be dependent on the number of protonated oxygen atoms involved in binding Ca^{2+} to the ATPase (Yu et al. 1994). Therefore, in conjunction with the experiments described here, we present a NET model of reconstituted Ca^{2+}-ATPase (accompanying paper in this issue) to: (1) make predictions about the extent of slip in the PM pump; and (2) guide the development of future experiments aimed at discerning membrane leak from ATPase slip.

Acknowledgements This work was supported by grants to each of P. W. K and B. D. R. from the Australian National Health and Medical Research Council. A. R. W. and A. S-L. X. acknowledge the support of a University of Sydney Postgraduate Research Award, and a CRC postdoctoral fellowship, respectively. We thank Dr. Tarik Kahn for purifying the human erythrocyte Ca^{2+}-ATPase.

References

Aiken NR, Satterlee JD, Galey WR (1992) Measurement of intracellular Ca^{2+} in young and old human erythrocytes using ^{19}F NMR spectroscopy. Biochim Biophys Acta 1136:155–160

Bachelard HS, Badar-Goffer RS, Brook KJ, Dolin SJ, Morris PG (1988) Measurement of free Ca^{2+} in the brain by ^{19}F-nuclear magnetic resonance spectroscopy. J Neurochem 51:1311–1313

Bubb W, Kirk K, Kuchel PW (1988) Ethylene glycol as a thermometer for X-nucleus spectroscopy in biological samples. J. Magn Reson 77:363–367

Deutsch C, Taylor JS (1989) New class of ^{19}F pH indicators: fluoroanilines. Biophys J 55:799–804

Erdahl WL, Chapman CJ, Taylor RW, Pfeiffer DR (1994) Ca^{2+} transport properties of ionophores A23187, ionomycin, and 4BrA23187 in a well defined model system. Biophys J 66:1678–1693

Erdahl WL, Chapman CJ, Taylor RW, Pfeiffer DR (1995) Effects of pH conditions on Ca^{2+} transport catalyzed by ionophores A23187, 4-BrA23187, and ionomycin suggest problems with common applications of these compounds in biological systems. Biophys J 69:2350-2363

Gilboa H, Chapman BE, Kuchel PW (1994) ^{19}F NMR magnetization transfer between 5FBAPTA and its complexes. NMR Biomed 7:330–338

Grandjean J, Laszlo P (1987) Cation transport across membranes: the NMR viewpoint. Biochem Life Sci 6:1–7

Hao L, Rigaud J-L, Inesi G (1994) Ca^{2+}/H^+ countertransport and electrogenicity in proteoliposomes containing erythrocyte plasma membrane Ca-ATPase and exogenous lipids. J Biol Chem 269:14268–14275

Karon BS, Nissen ER, Voss J, Thomas DD (1995) A continuous spectrophotometric assay for simultaneous measurement of calcium uptake and ATP hydrolysis in sarcoplasmatic reticulum. Anal Biochem 227:328–333

Kuchel PW, Kirk K, King GF (1994) In: Hilderson HJ, Ralston GB (eds) Physico-chemical methods in the study of biomembranes. Plenum Press, London, pp 247–327

Levy LA, Murphy E, London RE (1987) Synthesis and characterization of ^{19}F NMR chelators for measurement of cytosolic free Ca. Am J Physiol 252:C441–C449

Lundberg P, Harmsen E, Ho C, Vogel HJ (1990) Nuclear magnetic resonance studies of cellular metabolism. Anal Biochem 191:193–222

Metcalfe JC, Hesketh TR, Smith GA (1985) Free cytosolic Ca^{2+} measurements with fluorine labeled indicators using ^{19}F NMR. Cell Ca^{2+} 6:183–195

Mitchell P, Moyle J (1967) Acid-base titration across the membrane system of rat-liver mitochondria. Biochem J 104:588–600

Nicolay K, Kaptein R, Hellingwerf KJ, Konings WN (1981) ^{31}P nuclear magnetic resonance studies of energy transduction in *Rhodopseudomonas sphaeroides.* Eur J Biochem 116:191–197

Nicolay K, van Gemerden H, Hellingwerf KJ, Konings WN, Kaptein R (1983) *In vivo* ^{31}P and ^{13}C NMR studies of acetate metabolism in *Chromatium vinosum.* J Bact 155:634–642

Nishimura M, Ito T, Chance B (1962) A sensitive and rapid method of determination of photophosphorylation. Biochim Biophys Acta 59:177–182

Roufogalis BD, Villalobo A (1989) The $(Ca^{2+} + Mg^{2+})$-ATPase. Purification and reconstruction. In: Raess BU, Godfrey (eds) The red cell membrane. Humana Press, Clifton, New Jersey, pp 75–101

Simpson SJ, Bendall MR, Egan AF, Vink R, Rogers PJ (1983) High-field phosphorus NMR studies of the stoichiometry of the lactate/proton carrier in *Streptococcus faecalis.* Eur J Biochem 136:63–69

Steenbergen C, Murphy E, Levy L, London RE (1987) Elevation in cytosolic free Ca^{2+} concentration in early myocardial ischemia in perfused rat heart. Circ Res 60:700–707

Stewart IM, Chapman BE, Kirk K, Kuchel PW, Lovric VA, Raftos JE (1986) Intracellular pH in stored erythrocytes. Refinement and further characterisation of the ^{31}P-NMR methylphosphonate procedure. Biochim Biophys Acata 885:23–33

Szoka F, Papahadjopoulos D (1978) Procedure for preparation of liposomes with large internal aqueous space and high capture by reverse phase evaporation. Proc Natl Acad Sci 75:4194–4198

Villalobo A, Roufogalis BD (19869 Proton countertransport by the reconstituted erythrocyte Ca^{2+}-translocating ATPase: evidence using ionophoretic compounds. J Membr Biol 93:249–258

Vink R, Bendall MR, Simpson SJ, Rogers PJ (1984) Estimation of H^+ to 5′-triphosphate stoichiometry of *Escherichia coli* ATP synthase using ^{31}P NMR. Biochemistry 23:3667–3675

Waldeck AR, Kuchel PW (1993) ^{23}Na-nuclear magnetic resonance study of ionophore-mediated cation exchange between two populations of liposomes. Biophys J 64:1445–1455

Wang KKW, Roufogalis BD, Villalobo A (1989) Calpain I activates Ca^{2+} transport by the reconstituted erythrocyte Ca^{2+} pump. J Membr Biol 112:233–245

Xu AS-L, Kuchel PW (1991) Difluorophosphate as a ^{19}F NMR probe of erythrocyte membrane potential. Eur Biophys J 19:327–334

Yoon PS, Sharp RR (1985) Ca^{2+} and proton transport in chromaffin granule membranes: a proton NMR study. Biochemistry 24:7269–7273

Yu X, Carroll S, Rigaud J-L, Inesi G (1993) H^+ countertransport and electrogenicity of the sarcoplasmic reticulum Ca^{2+} pump in reconstituted proteoliposomes. Biophys J 64:1232–1242

Yu X, Hao L, Inesi G (1994) A p*K* change of acidic residues contributes to cation countertransport in the Ca-ATPase of sarcoplasmatic reticulum. J Biol Chem 269:16565–16661